# Gab1 Is an Integrator of Cell Death versus Cell Survival Signals in Oxidative Stress

Marina Holgado-Madruga* and Albert J. Wong*

*Department of Microbiology and Immunology, Kimmel Cancer Institute, Thomas Jefferson
University, Philadelphia, Pennsylvania 19107*

Upon the addition of different growth factors and cytokines, the Gab1 docking protein is tyrosine phosphorylated and in turn activates different signaling pathways. On the basis of the large body of evidence concerning cross talk between the signaling pathways activated by growth factors and oxidative stress, we decided to investigate the role of Gab1 in oxidative injury. We stimulated wild-type mouse embryo fibroblasts (MEF) or MEF with a homozygous deletion of the Gab1 gene ($-/-$ MEF) with $H_2O_2$. Our results show that Gab1 is phosphorylated in a dose- and time-dependent manner after $H_2O_2$ triggering. Gab1 then recruits molecules such as SHP2, phosphatidylinositol 3-kinase (PI3K), and Shc. Gab1 phosphorylation is sensitive to the Src family kinase inhibitor PP2. Furthermore, we demonstrate that Gab1 is required for $H_2O_2$-induced c-Jun N-terminal kinase (JNK) activation but not for ERK2 or p38 activation. Reconstitution of Gab1 in $-/-$ MEF rescues JNK activation, and we find that this is dependent on the SHP2 binding site in Gab1. Cell viability assays reveal that Gab1 has a dual role in cell survival: a positive one through its interaction with PI3K and a negative one through its interaction with SHP2. This is the first report identifying Gab1 as a component in oxidative stress signaling and one that is required for JNK activation.

Oxygen free radicals, also called reactive oxygen species (ROS), include a variety of chemical species such as superoxide anion, hydroxyl radical, and hydrogen peroxide. Their main characteristic is that they are highly reactive with cellular components. The origin of these species can be either exogenous or endogenous. Exogenous sources include those generated as a consequence of UV or ionizing radiation, chemotherapeutic agents, or hyperthermia. Endogenous ROS can be the result of physiological conditions (such as aerobic metabolism) or pathological situations (such as organ ischemia, Alzheimer's disease, and cancer). Nearly all organisms inactivate such ROS via a sophisticated enzymatic and nonenzymatic antioxidant system. The net balance between ROS production and antioxidant defenses determines the deleterious effects of oxidative stress on cellular proteins, lipids, and DNA (15).

Organisms have a variety of mechanisms for coping with ROS. When oxidative injury occurs there can be activation of a series of pathways to repair the ROS damage. Alternatively, there may be an attempt to adjust ROS levels, or in cases of sufficient damage, apoptosis is initiated to eliminate the damaged cells. The stress-induced proteins that are activated include tyrosine kinases such as epidermal growth factor (EGF) receptor (EGFR) (10, 50, 63, 72), platelet-derived growth factor (PDGF) receptor (PDGFR) (18, 28, 42), and Src (1, 37, 38, 48, 64, 69) and downstream pathways such as extracellular signal-regulated kinase (ERK) (20), c-Jun N-terminal kinase (JNK) (6, 52), p38 (11), phosphatidylinositol 3-kinase (PI3K), AKT (33, 63), the nuclear factor (NF)-κB system (27), p53 activation (9, 23, 29), and the heat shock response (43, 66). In

general, the heat shock response, ERK, PI3K/AKT, and NF-κB signaling pathways are prosurvival responses, whereas p53, JNK, and p38 activation is associated with apoptosis; however, exceptions should be considered a consequence of cellular specificity. The activation of these pathways is not unique to oxidative stress, since many of these same pathways are well accepted as playing an important role in cell growth and differentiation.

Gab1 was cloned in our laboratory (21) as a docking protein downstream of EGF and insulin receptor signaling. It has a pleckstrin homology (PH) domain at its N terminus, and the distal 2/3 parts are rich in proline and serine, resulting in 47 predicted serine/threonine phosphorylation sites. Significantly, it also has 16 potential tyrosine phosphorylation sites for the recruitment of Src homology 2 (SH2)-containing proteins. Upon the addition of growth factors and cytokines such as EGF, insulin, PDGF, hepatocyte growth factor (HGF), nerve growth factor, and the engagement of B- and T-cell receptors (5, 21, 22, 24, 35, 46, 47, 57, 65), Gab1 becomes tyrosine phosphorylated and recruits proteins, including Grb2, phospholipase Cγ (PLCγ), SHP2, PI3K, Shc, and Crk (21, 22, 24). Overexpression of Gab1 in NIH 3T3 fibroblasts increases cell growth and promotes transformation (21). PC12 cells and sympathetic neurons overexpressing Gab1 show protection of apoptosis induced by serum starvation (22, 35), and its overexpression in epithelial cells promotes tubulogenesis (65). Gab1 stimulates PI3K activity after the addition of growth factors (21, 22, 34, 35), and upon stimulation with HGF or engagement of GP130, it increases ERK activity (65). Gab1 leads to JNK activation (57) after EGF (51) or HGF (17) triggering.

Since Gab1 activates many of the same growth signaling pathways seen after ROS stimulation, we asked whether Gab1 also plays a role in oxidative stress signaling. To investigate this hypothesis, we have used normal (wild-type [Wt]) mouse em-

* Corresponding author. Mailing address: Kimmel Cancer Institute, Thomas Jefferson University, 233 S. 10th St., BLSB 1002, Philadelphia, PA 19107. Phone: (215) 503-4650. Fax: (215) 503-0567. E-mail for Albert J. Wong: albert.wong@mail.tju.edu. E-mail for Marina Holgado-Madruga: M_Holgado_Madruga@mail.jci.tju.edu.

bryo fibroblasts (Wt MEF), MEF that have been rendered deficient for the Gab1 gene by targeted disruption of both Gab1 alleles ($-/-$ MEF), and fibroblasts heterozygous for the Gab1 gene ($-/+$ MEF). Our findings show that Gab1 is phosphorylated in a dose- and time-dependent manner after $H_2O_2$ addition. It recruits molecules such as SHP2, PI3K, and Shc. Gab1 tyrosine phosphorylation status is sensitive to the Src family kinase inhibitor PP2. Furthermore, we demonstrate that Gab1 is specifically required for $H_2O_2$-induced JNK activation but not for activation of JNK by other stimuli. Gab1 is also not required for ERK2 or p38 activation after $H_2O_2$ addition. Reconstitution of Gab1 in $-/-$ MEF rescues JNK activation, and this is dependent on the SHP2 binding site in Gab1. Viability assays show that Gab1 is required for maintaining cell survival after oxidative stress in a dual manner, positively through its interaction with PI3K and subsequent AKT activation and negatively through its interaction with SHP2 which leads to JNK activation. Thus, we have identified Gab1 as an important component in oxidative stress signaling with an essential role in the activation of JNK and the influencing of cell survival.

## MATERIALS AND METHODS

**Materials.** Hydrogen peroxide ($H_2O_2$) was purchased from Sigma, and EGF and PDGF were obtained from Invitrogen Corp. AG1478, AG1296, PP2, SU6656, and wortmannin were all purchased from Calbiochem. The anti-SHP2, anti-Shc, and anti-PDGFR antibodies were from Transduction Laboratories. The anti-phosphotyrosine, anti-Src, and anti-PI3K antibodies were from Upstate Biotechnology, Inc. The antibodies against ERK2, p38, and JNK1 were purchased from Santa Cruz Biotechnology, Inc. The anti-EGFR antibody was from Promega. Anti-Gab1 antibody was raised in rabbits by immunization with a glutathione $S$-transferase (GST)–Gab1 fusion protein as described previously (21). The anti-AKT and phospho-AKT antibodies were from Cell Signaling Technology, Inc., and the antihemagglutinin (anti-HA) was from Covance Inc. The anti-Met antibody was a generous gift from Morag Park. The anti-rabbit and anti-mouse antibodies, ECL reagent, and protein G-Sepharose were from Amersham Pharmacia Biotech. GST–c-Jun, myelin basic protein (MBP), and GST-ATF2 were from Upstate Biotechnology, Inc. All other materials were from Fisher Scientific unless otherwise indicated.

**Generation of Gab1-deficient mice.** 129SV/J mouse genomic DNA was sequenced to determine the intron-exon boundaries. A 4.0-kb genomic fragment 5′ of the second exon, which contains part of the PH domain, and a 4.5-kb fragment 3′ of this exon were obtained by PCR. Details of the sequences and primers are available upon request. The 4.0- and 4.5-kb fragments were cloned proximally and distally, respectively, to the neomycin resistance gene in a vector which also contains the diphtheria toxin gene for negative selection of nonhomologous recombinants. Transfected embryonic stem cell colonies that survived after selection with G418 were subcloned, and using primers and probes located on both sides of exon 2, homologous recombination events were detected by both PCR and Southern blotting. Targeted cells were injected into C57BL/6 mouse blastulas to create chimeric male founders, which were mated to C57BL/6 mice to generate $F_1$ heterozygous progeny. The $F_1$ progeny were then intercrossed to generate $F_2$ progeny. $F_1$ heterozygous males were crossed with $F_1$ or $F_2$ heterozygous females to generate embryos with a homozygous disruption of Gab1. The genotypes of the embryos were identified by a combination of Southern blotting, PCR, and Western blotting. The Gab1$^{-/-}$ mice died in utero between embryonic day 13.5 (E13.5) and E18.5 and showed developmental defects in the heart, placenta, and skin, phenotypes which are similar to those previously reported for Gab1$^{-/-}$ mice (25).

**Cell lines, cell cultures, and transfections.** HeLa, H460, and U87 cells were originally obtained from the American Type Culture Collection. Cell cultures were grown in Dulbecco's modified Eagle's medium (DMEM) supplemented with 10% calf serum, 100 U of penicillin/ml, 100 μg of kanamycin/ml, and 100 μg of streptomycin/ml. Wt MEF and fibroblasts rendered deficient for Gab1 ($-/-$ MEF) or heterozygous for Gab1 ($-/+$ MEF) were derived from fibroblasts of embryos from crosses between Gab1$^{-/+}$ mice. Females were sacrificed on day 13 of pregnancy, the embryos were dissected from the uterus in phosphate-buffered

saline (PBS), and the yolk sac, amnion, and placenta were removed. The embryos were washed in PBS to eliminate any blood, and the head and liver were pinched off. The carcasses were placed in the barrel of a sterile 3-ml syringe with an 18-gauge hypodermic needle, and PBS was added. They were expelled and drawn through the needle four to five times to break them into smaller clumps of cells and then seeded into a dish containing DMEM supplemented with 10% calf serum, 100 U of penicillin/ml, 100 μg of kanamycin/ml, and 100 μg of streptomycin/ml (Invitrogen). The plates were transferred to 37°C in a 5% $CO_2$ incubator. Adherent cells were allowed to reach confluence once and then passaged according to the 3T3 protocol (67).

The reconstitution of Gab1 wild-type cDNA ($-/-$ MEF/Gab1), Gab1/ΔSHP2 cDNA ($-/-$ MEF/Gab1/ΔSHP2), and Gab1/ΔPI3K cDNA ($-/-$ MEF/Gab1/ΔPI3K) into $-/-$ MEF cells was performed using the PMSCV retroviral expression vector which contains a hygromycin-resistant cassette (Clontech). Constructs contained a HA tag at the amino-terminal end of Gab1, and two artificial BHI-$Eco$RI sites were engineered to insert this fragment into the $Xho$I and $Hpa$I sites in the vector. The generation of Gab1/ΔSHP2 cDNA (a Gab1 cDNA with a Y628F substitution) and Gab1/ΔPI 3-kinase cDNA (a Gab1 cDNA lacking the three binding sites for PI 3-kinase, Y448F, Y473F, and Y590F) was performed as described elsewhere (21, 22, 41). Phoenix cells were transfected with 20 μg of plasmid DNA in a 10-cm-diameter dish. Cells were refed at 12 to 16 h after transfection, and Polybrene (8 μg/ml)-supplemented virus-containing supernatant was transferred to $-/-$ MEF at 48 h after transfection. After an overnight infection period, fibroblasts were refed. Selection was started by using 500 mg of hygromycin (Roche)/ml at 48 h after infection (67).

$-/-$ MEF/Gab1 cells were transiently cotransfected with an empty vector, an expression vector containing a deletion within the SH2 domain of the regulatory subunit of PI3K (DNp85; a gift from P. Tschilis) (7), or an expression vector containing a catalytically inactive form of SHP2 (SHP2 C/S; a gift from S. Reeves) (53) together with a farnesylated form of pEGFP (pEGFP-F) (Clontech) as a marker for transfection efficiency. Cells were seeded on 35-mm-diameter dishes and transfected 24 h later with a total amount of 2 μg by using a 1/20 ratio of green fluorescent protein F (GFP-F) relative to each construct and 8 μl of Fugene-6 (Roche). Transfection efficiency was monitored by immunofluorescence microscopy and fluorescence-activated cell sorter (FACS) analysis.

**Immunoprecipitation and Western analysis.** Cells were serum starved for 48 h and stimulated in DMEM containing the various concentrations of $H_2O_2$. In the cases indicated, cells were preincubated with different inhibitors (100 nM AG1478, 10 μM AG1296, 200 nM wortmannin, or 25 μM PP2) or dimethyl sulfoxide (DMSO) as a vehicle at 30 min prior to stimulation with $H_2O_2$. Cells were then washed in ice-cold PBS and lysed using a buffer containing 10 mM $Na_2HPO_4$, 150 mM NaCl, 1% Triton X-100, 0.5% sodium deoxycholate, 0.1% sodium dodecyl sulfate, 0.2% sodium azide, 0.004% sodium fluoride, 1 mM $NaVO_4$, 25 mM β-glycerophosphoric acid, 100 μg of phenylmethanesulfonyl fluoride/ml, 10 μg of aprotinin/ml, and 10 μg of leupeptin/ml (pH 7.35). Lysates were clarified by centrifugation at $12,000 \times g$ for 10 min at 4°C. Protein concentrations were determined using the Bio-Rad DC protein assay. Cell lysates were combined with antibody previously bound to 30 μl of a 50% slurry of protein G-Sepharose overnight at 4°C. Immunoprecipitates were washed three times with the same lysis buffer and resuspended in sample buffer. Immunocomplexes and whole lysates were resolved on 4 to 12% Tris-glycine gels (Novex) and transferred to nitrocellulose membranes (Schleicher & Schuell). The membranes were blocked in TTBS–5% Blotto (100 mM Tris [pH 7.5], 0.9% NaCl, 0.1% Tween 20 with 5% nonfat dry milk) and incubated with the different antibodies (44). Proteins were detected by using ECL reagents (Amersham Pharmacia Biotech).

**Kinase assays (JNK, ERK, and p38).** After stimulation with $H_2O_2$, cells were lysed in the same lysis buffer as described above. Cell lysates were combined with immunocomplexes containing 30 μl of a 50% slurry of protein G-Sepharose and 1 μg of anti-JNK1 (for the JNK kinase assay), anti-ERK2 (for the ERK2 kinase assay), or anti-p38 antibody (for the p38 kinase assay) for 2 h at 4°C. Immunoprecipitates were washed three times with PBS containing 1% Nonidet P-40 and 2 mM $NaVO_4$ and once with kinase reaction buffer (25 mM HEPES, 25 mM $MgCl_2$, 2 mM dithiothreitol, 0.1 mM $NaVO_4$, 25 mM β-glycerophosphoric acid). The pellet was incubated in 30 μl of kinase reaction buffer containing 20 μM unlabeled ATP, 5 μCi of [γ-$^{32}$P]ATP, and 1 μg of substrate (GST–c-Jun for the JNK kinase assay, MBP for the ERK assay, and GST-ATF2 for the p38 kinase assay) at 30°C for 20 min (2, 39, 68). Samples were separated on a 12% Tris-glycine gel, transferred onto nitrocellulose, and exposed on a PhosphorImager cassette for quantification using ImageQuant software (Molecular Dynamics, Inc., Sunnyvale, Calif.).

**Cell viability assays.** For studies with stable cell lines, cells were seeded in duplicate in 35-mm-diameter dishes to reach 80 to 90% confluence at 12 to 16 h

later. Then, cells were either not treated (DMEM control group) or were stimulated with DMEM containing 600 $\mu$M $H_2O_2$ for up to 3 days. Cells were harvested and stained with trypan blue, and live cells were counted using a hemocytometer. The percentage of viable cells in the treatment group was determined by dividing the cell count for the treatment group by the cell count for the untreated control group (64). For studies with transiently transfected cell lines, cells were seeded in duplicate on 35-mm-diameter dishes. At 24 h after cotransfection of the different constructs together with the pEGFP-F vector, the cells were either left untreated (DMEM control group) or treated with 600 $\mu$M $H_2O_2$ for up to 3 days. Cells were harvested, washed twice with ice-cold PBS containing 5 mM EDTA, and fixed in 70% ethanol. The use of a farnesylated form of pEGFP prevented the leakage of the fluorescent protein after permeabilization with ethanol. Samples were stored at $-20$°C until the day of analysis. At that time, cells were pelleted, washed with ice-cold PBS with 5 mM EDTA, and finally resuspended in staining solution containing 50 $\mu$g of propidium iodide (Sigma)/ml and 80 $\mu$g of DNase-free RNase (Roche)/ml in PBS. The level of cell death was estimated by FACS analysis (using a FACSCalibur flow cytometer and CellQuest software; Becton Dickinson) based on the sub-$G_0/G_1$ DNA content of the GFP-positive cells (30).

## RESULTS

**Gab1 is tyrosine phosphorylated after $H_2O_2$ addition in a dose- and time-dependent manner in different cell lines.** It has been well established that Gab1 is tyrosine phosphorylated and participates in different signaling pathways after the addition of multiple growth factors or cytokines (5, 21, 22, 24, 35, 47, 57) or osmotic stress (26). We hypothesized that Gab1 is involved in the response to ROS. To study the status of Gab1 phosphorylation after the addition of $H_2O_2$, Wt MEF were stimulated with increasing concentrations of $H_2O_2$ for 30 min, lysed, and immunoprecipitated with anti-Gab1 antibody. Western blots were incubated with antiphosphotyrosine antibody. We chose a 30-min interval for stimulation, since this duration has been widely used for the study of signaling proteins after $H_2O_2$ stimulation (64). As shown in Fig. 1A, Gab1 becomes tyrosine phosphorylated in a dose-dependent manner at concentrations as low as 600 $\mu$M $H_2O_2$. Next, we investigated the time course of Gab1 phosphorylation. Gab1 becomes phosphorylated within 5 min, reaches a peak at 10 min, and then returns to basal levels within 1 h (Fig. 1B). Blotting with anti-Gab1 antibody confirmed that there were equal amounts of Gab1 in all lanes. Since ROS have been implicated in the pathogenesis of cancer, we sought to analyze the status of Gab1 phosphorylation after $H_2O_2$ addition in cancer cell lines. HeLa, H460, and U87 cells were stimulated for 10 min with 600 $\mu$M $H_2O_2$. Lysates were subjected to immunoprecipitation with anti-Gab1 antibody followed by Western blotting analysis with antiphosphotyrosine antibody. Figure 1C shows that an increase in Gab1 phosphorylation occurred after $H_2O_2$ triggering in all cell lines, indicating that Gab1 can be phosphorylated in these cells. Western blotting with anti-Gab1 antibody showed equal amounts of Gab1 in the cell lines.

**Gab1 tyrosine phosphorylation after $H_2O_2$ stimulation is sensitive to the Src family kinase inhibitor PP2.** It has been reported that the EGFR (10, 50, 63, 72) and PDGFR (18, 28, 42) participate in signaling events in response to oxidative injury. Because Gab1 is tyrosine phosphorylated after EGF (21, 21) or PDGF addition (47), we sought to investigate the role of these receptors in Gab1 phosphorylation after $H_2O_2$ stimulation. Wt MEF cells were preincubated for 30 min with 100 nM AG1478 (a selective inhibitor of the kinase activity of the EGFR) or 10 $\mu$M AG1296 (a selective inhibitor of the
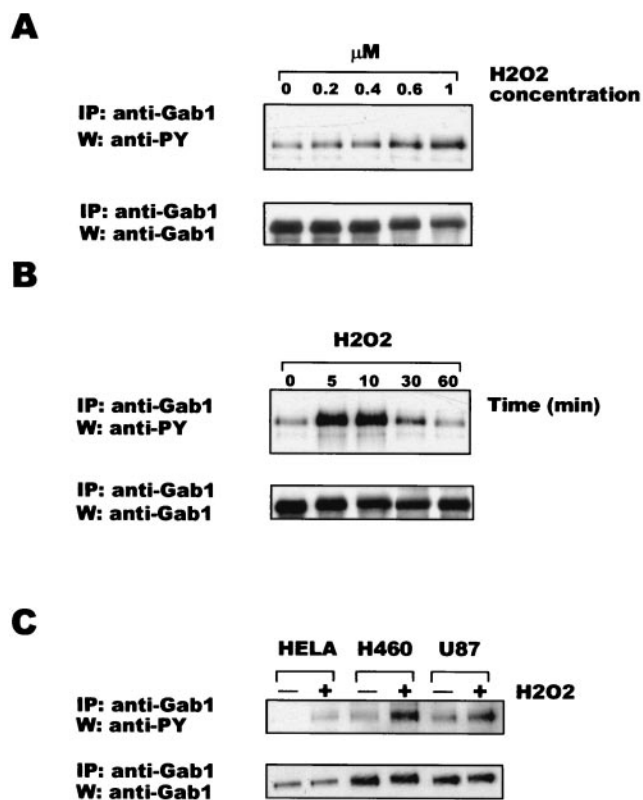


FIG. 1. Gab1 is tyrosine phosphorylated after $H_2O_2$ addition in a dose- and time-dependent manner in different cell lines. (A) Wt MEF cells were incubated with increasing concentrations of $H_2O_2$ for 30 min. (Upper panel) Immunoprecipitations with anti-Gab1 antibody were performed on cell lysates, and the resulting Western blots were incubated with anti phosphotyrosine antibody (anti-PY). (Lower panel) The same membrane was reincubated with anti-Gab1 antibody. (B) Wt MEF cells were triggered with 600 $\mu$M of $H_2O_2$ for the indicated periods of time. (Upper panel) Immunoprecipitations with anti-Gab1 antibody and Western analysis with antiphosphotyrosine antibody were performed as described above. (Lower panel) Western blotting with anti-Gab1 antibody was performed with the same membrane. (C) HeLa, H460, and U87 cells were stimulated with 600 $\mu$M $H_2O_2$ for 10 min. Immunoprecipitations and Western blotting were done as described for panels A and B. Experiments were repeated three times; data from one representative assay are shown. IP, immunoprecipitation; W, Western blotting.

kinase activity of the PDGFR) prior to stimulation with 600 $\mu$M $H_2O_2$ for 10 min. Immunoprecipitations with anti-Gab1 antibody were followed by Western blotting with antiphosphotyrosine antibody. Neither AG1478 nor AG1296 modified the phosphorylation status of Gab1 (Fig. 2A). As shown in Fig. 2B and C, respectively, we confirmed that the AG1478 and AG1296 inhibitors were indeed functional.

The PI3K/AKT pathway is activated in response to $H_2O_2$ treatment (14, 63). Recent results have revealed a novel positive-feedback loop in which PI3K functions as both an upstream regulator and a downstream effector of Gab1 in signaling via the EGFR (51). We wished to test the role of PI3K in the phosphorylation of Gab1 by $H_2O_2$ by using wortmannin as a PI3K inhibitor. Cells were pretreated for 30 min with 200 nM wortmannin before stimulation with 600 $\mu$M $H_2O_2$ for 10 min, and samples were processed as described above. This treat-
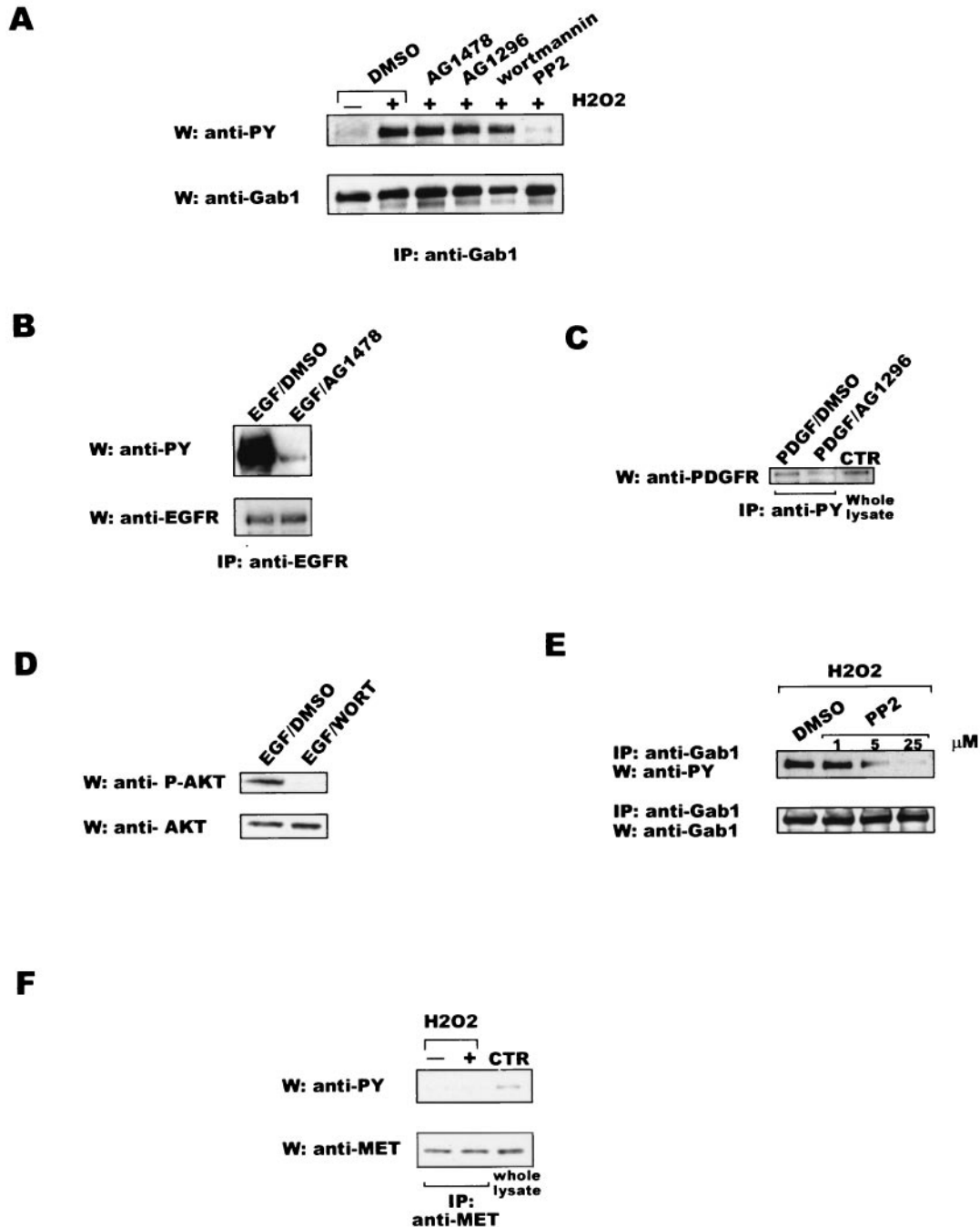
FIG. 2. Gab1 tyrosine phosphorylation after $H_2O_2$ stimulation is sensitive to the Src family kinase inhibitor PP2. (A) Wt MEF cells were preincubated for 30 min with the different inhibitors (100 nM AG1478, 10 μM AG1296, 25 μM PP2, or 200 nM wortmannin) or DMSO as the vehicle control and then stimulated with 600 μM of $H_2O_2$ for 10 min. (Upper panel) Cell lysates were subjected to immunoprecipitation with anti-Gab1 antibody followed by Western blotting with antiphosphotyrosine antibody (anti-PY). (Lower panel) The same membrane was reincubated with anti-Gab1 antibody. (B) Wt MEF cells were pretreated for 30 min with 100 nM AG1478 or DMSO and then stimulated with EGF (100 ng/ml) for 10 min. (Upper panel) Immunoprecipitation with anti-EGFR antibody was followed by immunoblotting with antiphosphotyrosine antibody. (Lower panel) The same membrane was reincubated with anti-EGFR antibody. (C) Wt MEF cells were pretreated for 30 min with 10 μM AG1296 or DMSO prior to stimulation with 50 ng of PDGF/ml for 10 min. Immunoprecipitation with antiphosphotyrosine antibody was followed by Western blotting with anti-PDGFR. Whole lysate was run as a control for PDGFR antibody (CTR). (D) Wt MEF cells were preincubated with 200 nM wortmannin (WORT) or DMSO prior to stimulation with 100 ng of EGF/ml for 10 min. (Upper panel) Western blotting was performed with anti-phospho-AKT antibody (anti-P-AKT). (Lower panel) The membrane was stripped and reincubated with anti-AKT antibody. (E) Wt MEF cells were preincubated with different concentrations of PP2 or DMSO for 30 min and then stimulated with 600 μM $H_2O_2$ for 10 min. (Upper panel) Lysates were subjected to immunoprecipitation (ip) with anti-Gab1 antibody followed by Western blotting analysis with antiphosphotyrosine antibody. (Lower panel) The same membrane was reincubated with anti-Gab1 antibody. (F) HeLa cells were stimulated with 600 μM $H_2O_2$ for 10 min. Immunoprecipitation assays with anti-Met antibody were performed on lysates. Western blotting analysis was done with either antiphosphotyrosine antibody (upper panel) or anti-Met antibody (lower panel). Experiments were repeated three times; data from one representative assay are shown. IP, immunoprecipitation; W, Western blotting.

ment showed no effect on Gab1 phosphorylation after $H_2O_2$ addition (Fig. 2A), despite the fact that wortmannin inhibited the EGF-induced AKT activation (Fig. 2D).

Src family kinases have also been implicated in signaling events stimulated by ROS (1, 37, 38, 48, 64, 69). Since Gab1 phosphorylation has been shown to be regulated by Src family members in other systems (12, 26, 55), we were interested in investigating the role of these kinases in Gab1 phosphorylation after $H_2O_2$ addition. Pretreatment of the cells with 25 μM PP2 (a selective inhibitor of Src family kinases) was followed by stimulation with 600 μM $H_2O_2$ for 10 min. Immunoprecipitations and Western blotting analysis were performed as previously described. As depicted in Fig. 2A, PP2 reduced the phosphorylation of Gab1 after $H_2O_2$ incubation. To further validate this hypothesis, we pretreated the cells with different concentrations of PP2 followed by $H_2O_2$ stimulation. As shown in Fig. 2E, we were able to detect a reduction in Gab1 phosphorylation in a dose-dependent manner. Similar results were obtained by using 1 μM SU6656, another inhibitor of Src family kinases (data not shown).

Since Gab1 is the major substrate for the Met receptor, we wished to investigate whether this kinase can regulate Gab1 phosphorylation in ROS signaling. HeLa cells were stimulated with 600 μM $H_2O_2$ for 10 min. Lysates were subjected to immunoprecipitation with anti-Met antibody followed by Western blotting analysis with antiphosphotyrosine antibody. Figure 2F reveals the absence of phosphorylation of the Met receptor under these conditions (upper panel), despite the presence of this kinase as shown by Western blotting of the immunocomplexes with anti-Met antibody (lower panel). Thus, Met is not likely to participate in the $H_2O_2$-induced phosphorylation of Gab1.

**Downstream effectors of Gab1 after $H_2O_2$ stimulation.** Since Gab1 behaves as a docking protein to recruit SH2-containing proteins after phosphorylation by different tyrosine kinase receptors (21, 22, 24, 46, 65), we asked whether Gab1 serves the same function after $H_2O_2$ addition. Wt MEF cells were stimulated with $H_2O_2$ for 10 min, and anti-Gab1 immunoprecipitates were subjected to Western blot analysis with antibodies against different SH2-containing proteins. As shown in Fig. 3, we were able to detect an increase in Gab1 association for PI3K, SHP2, and Shc. Because we have observed that Gab1 is phosphorylated by Src, we asked whether these two molecules were in the same complex. Figure 3 shows that despite a role for Gab1 phosphorylation by Src, they did not associate in a complex. We were also unable to detect an increase in the binding of Gab1 to PLCγ or Crk after $H_2O_2$ incubation (data not shown), whereas binding can be found after growth factor stimulation (21, 24).

**Gab1 is required for JNK activation by $H_2O_2$.** The JNK pathway has been described as being activated during oxidative stress signaling (6, 52) and plays an important role in the promotion of apoptosis. As Gab1 has been shown to participate in JNK activation in growth factor signaling (17, 51), we tested whether Gab1 was required for JNK activation after $H_2O_2$ addition. For this purpose we generated Gab1-deficient mice and developed fibroblasts deficient for the Gab1 gene (−/− MEF) and fibroblasts heterozygous for the Gab1 gene (−/+ MEF). The design of the targeting vector is presented in Fig. 4A. The level of Gab1 expression in these cell lines is
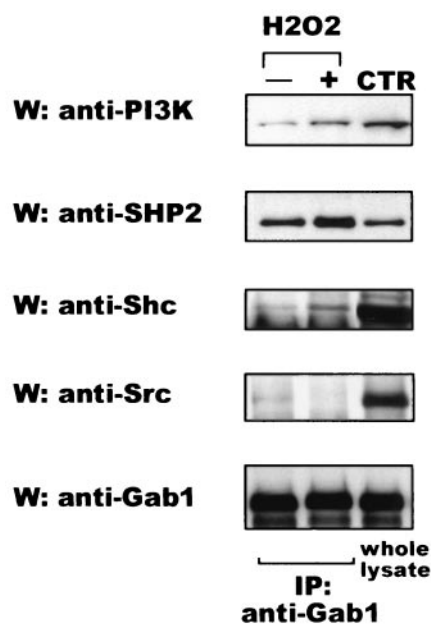


FIG. 3. Downstream effectors of Gab1 after $H_2O_2$ stimulation. Wt MEF were stimulated with 600 μM of $H_2O_2$ for 10 min. Gab1 was immunoprecipitated (IP) from cell lysates with anti-Gab1 antibody and immunocomplexes were subjected to Western blot analysis (W) with specific antibodies against the different molecules (anti-PI3K, anti-SHP2, anti-Shc, anti-Src, and anti-Gab1) as indicated. Whole lysate was run as a control for the antibodies (CTR). The experiments were repeated three times; data from one representative assay are shown.

depicted in Fig. 4B. These cells express similar levels of JNK1 protein (Fig. 4C). Wt MEF and −/− MEF cells were stimulated with 600 μM $H_2O_2$ for up to 60 min. Lysates were immunoprecipitated using anti-JNK1 antibody, and JNK kinase assays were performed using GST–c-Jun as the substrate. Remarkably, we found a reduction of JNK activation in two different sets of −/− MEF cell lines in comparison with that seen in Wt MEF cell lines (Fig. 4D). To see whether there is any effect attributable to gene dosage levels, the same experiment was performed using Wt MEF, −/− MEF, and −/+ MEF cells stimulated with 600 μM $H_2O_2$ for 30 min. Figure 4E revealed intermediate levels of JNK activation in −/+ MEF cells in comparison with that seen in Wt MEF cells and −/− MEF cells, supporting the idea of a dose effect for Gab1 in the activation of this kinase. Interestingly, this effect was highly specific for $H_2O_2$ since no differences in JNK activation were observed between these cell lines after stimulation with other activators of JNK, such as nocodazole, anisomycin, and sorbitol (61, 71) (Fig. 4F).

**Gab1 is not required for the activation of other MAPKs.** It has been reported that other mitogen-activated protein kinases (MAPKs) such as ERK2 (20) and p38 (11) are activated upon $H_2O_2$ stimulation. Since Gab1 is required for JNK activation after $H_2O_2$ addition and for ERK2 activation after the addition of certain growth factors (25), we wanted to explore whether it functions in the same manner for other MAPKs in oxidative stress. Stimulation of Wt and −/− MEF cells with 600 μM $H_2O_2$ was followed by immunoprecipitation with anti-ERK2 antibodies (for the ERK2 kinase assays) or with anti-p38 an-

tibodies (for the p38 kinase assays), and the kinase reaction was performed using MBP as a substrate (for the ERK2 kinase assays) or GST-ATF2 (for the p38 kinase reaction). We were not able to detect differences in ERK2 (Fig. 5A) or p38 (Fig. 5C) activation between the Wt and −/− MEF in two different sets of cell lines. Western analysis revealed similar levels of ERK2 (Fig. 5B) and p38 (Fig. 5D) expression in the cell lines studied. These data demonstrate that Gab1 is specifically required for JNK but not for ERK2 or p38 activation after $H_2O_2$ incubation.

**Reconstitution of Gab1 expression in −/− MEF cells rescues JNK activation after $H_2O_2$ stimulation and is dependent on the SHP2 binding site in Gab1.** To verify that the results seen were not due to clonal differences in the MEF lines examined, we investigated the effect of reconstituting Gab1 expression back into the −/− MEF cells. Stable cell lines were generated by retroviral transfection with a hygromycin-resistant vector containing HA-tagged Gab1 cDNA (−/− MEF/Gab1) or empty vector (−/− MEF/CTR). Figure 6A and B show Gab1 expression and Gab1 phosphorylation, respectively, in −/− MEF/Gab1 cells. JNK assays were performed as described above, and the results presented in Fig. 6C show that the reintroduction of Gab1 into these cells (−/− MEF/Gab1) was able to rescue JNK activation in comparison with control cells (−/− MEF/CTR) after $H_2O_2$ addition. This result demonstrates that the expression of Gab1 is essential for $H_2O_2$-induced JNK activation. We then wished to investigate which of the proteins that interact with Gab1 mediate JNK activation. It has been reported that SHP2 is important for JNK activation by insulin (16). To examine whether this interaction is relevant to $H_2O_2$ stimulation, we mutated one binding site in Gab1 for SHP2 and introduced this construct (Gab1/ΔSHP2) into the −/− MEF (−/− MEF/Gab1/ΔSHP2) cell line. This cell line has a level of Gab1 expression similar to −/− MEF/Gab1 (Fig. 6A) as well as a similar status of tyrosine phosphorylation upon $H_2O_2$ stimulation (Fig. 6B). As expected, −/− MEF/Gab1/ΔSHP2 cells did not show SHP2 binding after $H_2O_2$ addition (Fig. 6B, middle panel). JNK assays were performed, and as shown in Fig. 6C, −/− MEF/Gab1/ΔSHP2 cells were not able to activate JNK after $H_2O_2$ addition despite levels of JNK1 protein similar to those of −/− MEF/Gab1 cells (Fig. 6D). The Gab1/PI3K interaction has been shown to be necessary for JNK activation following EGF stimulation (51). However, we did not find definitive evidence that this interaction was nec-

essary for JNK activation after $H_2O_2$ stimulation (data not shown).

**Dual role of Gab1 in maintaining cell viability after $H_2O_2$ addition.** $H_2O_2$ functions in a dose-dependent manner to induce apoptosis in different cell types (32, 56, 60, 62). To explore the role of Gab1 in cell survival after $H_2O_2$ addition, Wt MEF and fibroblasts rendered deficient for Gab1 (−/− MEF) were either left untreated or treated with DMEM containing 600 μM $H_2O_2$ for a period of up to 3 days. Trypan blue exclusion was used to assess viability. As shown in Fig. 7A, −/− MEF cells were more sensitive to the deleterious effect of $H_2O_2$ than Wt MEF cells. Within 4 to 8 h, the −/− MEF cells began to shrink, and viability decreased to ∼5% after 24 h. In comparison, the Wt MEF cells had a more flattened appearance, with ∼45% survival after the first day. To prove a direct role for Gab1 in viability, we performed the same experiment using −/− MEF/Gab1 cells. Figure 7B shows that the −/− MEF/Gab1 cells were highly resistant to cell death in comparison with the knockout MEF cells (−/− MEF/CTR), with viability similar to Wt MEF cells.

Several pathways have been implicated in controlling cellular sensitivity to oxidant injury. Prominent among those linked to apoptosis after oxidative stress is the JNK pathway. Since we were able to show that −/− MEF/Gab1/ΔSHP2 cells are unable to activate JNK upon $H_2O_2$ triggering, we asked whether these cells are protected from oxidative injury. As expected, −/− MEF/Gab1/ΔSHP2 cells did show resistance to $H_2O_2$-induced cell death but, surprisingly, had higher levels of viability than −/− MEF/Gab1 cells, especially after the second and third day (Fig. 7B). This observation led us to investigate additional pathways initiated by Gab1 that are responsible for cell survival. The PI3K/AKT pathway has been reported to protect cells from oxidative stress-induced cell death (33, 63). We asked how the Gab1/PI3K interaction affected cell survival after ROS stress. We transfected Gab1/ΔPI3K cDNA into −/− MEF cells (−/− MEF/Gab1/ΔPI3K) and performed viability assays. −/− MEF/Gab1/ΔPI3K cells had a level of Gab1 expression as well as levels of tyrosine phosphorylation upon $H_2O_2$ addition similar to −/− MEF/Gab1 cells. As expected, −/− MEF/Gab1/ΔPI3K cells did not show any binding to PI3K upon $H_2O_2$ stimulation (Fig. 7C). After $H_2O_2$ incubation, the −/− MEF/Gab1/ΔPI3K cells showed enhanced sensitivity to this agent and a level of cell death comparable to that observed in −/− MEF/CTR cells (Fig. 7B).

FIG. 4. Gab1 is required for JNK1 activation by $H_2O_2$. (A) Diagram showing the targeting vector for the generation of Gab1-deficient mice. A restriction map of the first three exons of the Gab1 gene (top), the replacement targeting vector (middle), and a map of the locus after homologous recombination (bottom) are shown. The targeting vector replaces exon 2, which encodes the latter half of the PH domain, with the neomycin resistance gene (neo) and uses the diphtheria toxin gene (Dtx.) for negative selection of embryonic stem cell clones. (B) Western blotting (W) was performed with anti-Gab1 antibody to show the level of expression of Gab1 in the cell lines used. (C) Western blot analysis (W) was performed on lysates from two different sets of Wt, −/−, and −/+ MEF cell lines with anti-JNK1 antibody. (D) (Upper panel) Wt MEF and −/− MEF cells were stimulated with 600 μM of $H_2O_2$ for the indicated periods of time, and JNK assays were performed as described in Materials and Methods. (Lower panel) The kinase assay was quantified by PhosphorImager analysis using ImageQuant software, and the results are reported using the arbitrary units assigned by the PhosphorImager (means ± standard deviations [SD] are shown; $n = 2$). (E) (Upper panel) Wt MEF, −/−, and −/+ MEF cells were stimulated for 30 min, and JNK assays were performed as described above. (Lower panel) Quantification of the kinase assay (means ± SD are shown; $n = 2$) is shown. (F) (Left panel) Wt MEF and −/− MEF cells were incubated with anisomycin (Aniso) (10 μg/ml), nocodazole (Noco) (0.5 μg/ml), or sorbitol (Sorb) (500 mM) for 30 min, and JNK assays were performed as described above. Quantification of the kinase assay (means ± SD are shown; $n = 2$) is shown in the right panel. Experiments were done in duplicate three times with two different sets of cell lines; data from one representative assay are shown.
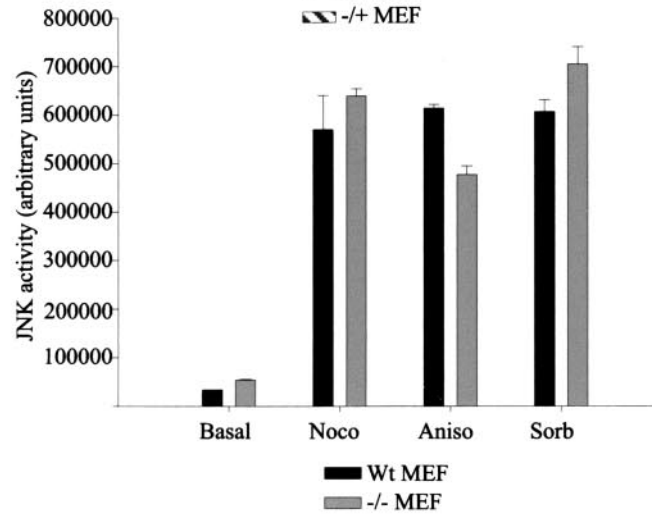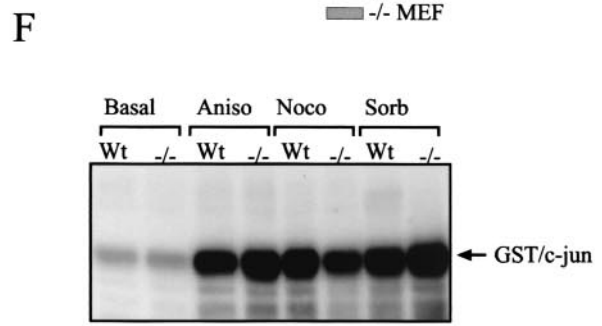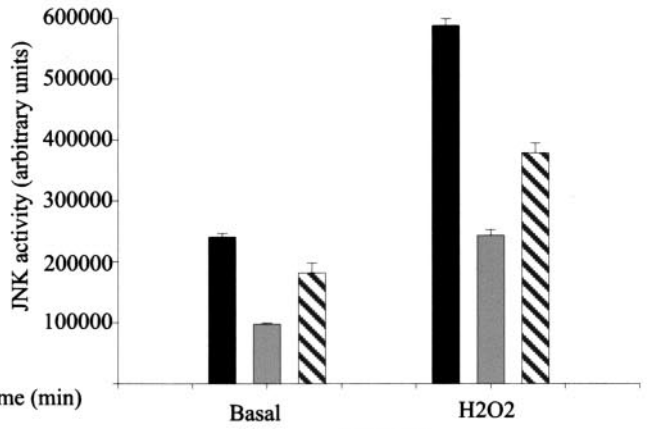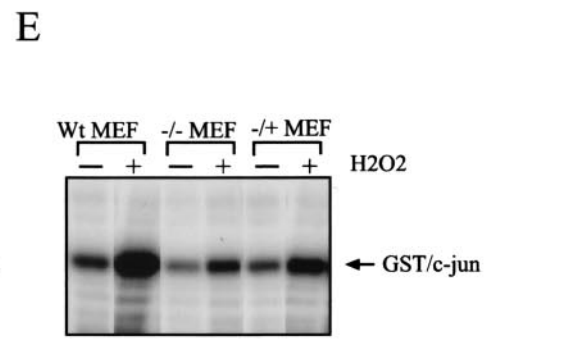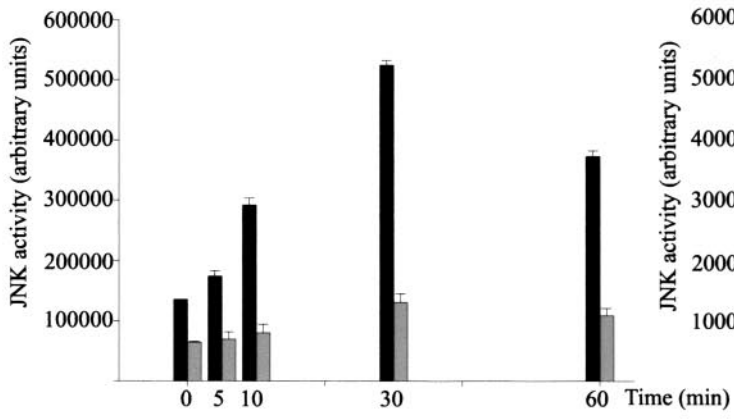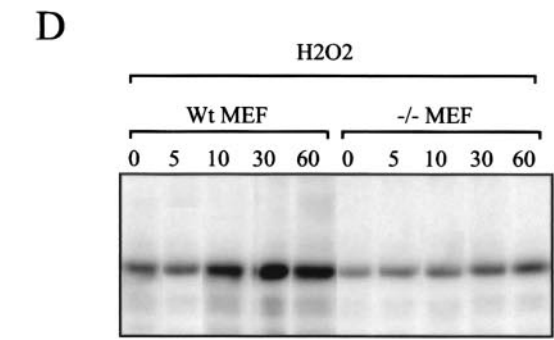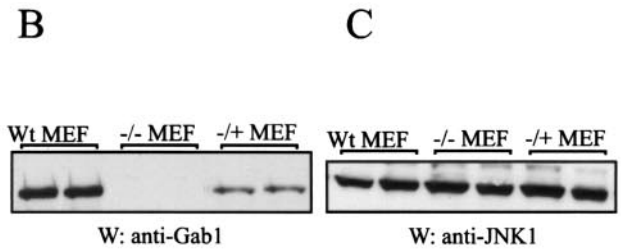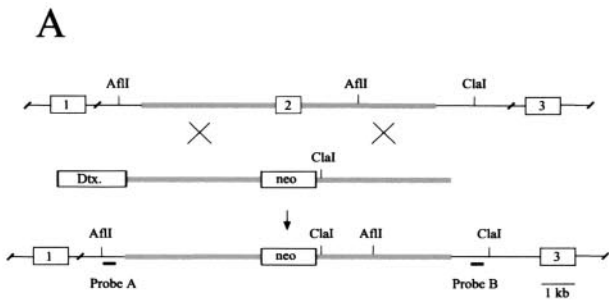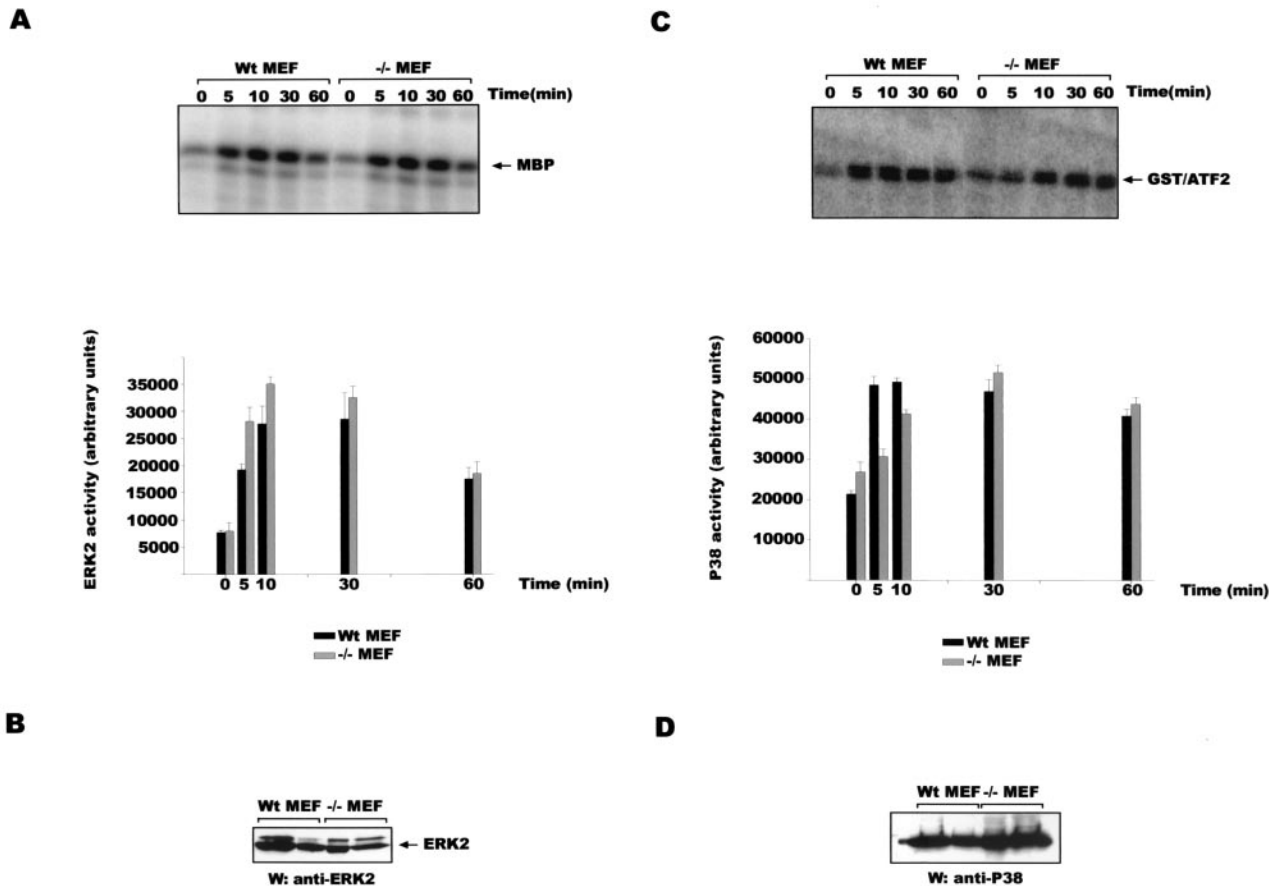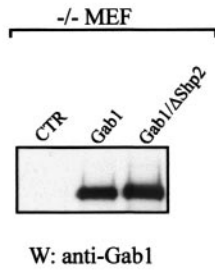
FIG. 5. Gab1 is not required for ERK2 or p38 activation after $H_2O_2$ addition. (A) (Upper panel) Wt and $-/-$ MEF cells were stimulated with 600 $\mu$M of $H_2O_2$ for the times indicated, and ERK2 kinase assays were performed as described in Materials and Methods. (Lower panel) The assay was quantified by PhosphorImager analysis, and the results are reported using the arbitrary units assigned by the PhosphorImager (means $\pm$ SD are shown; $n = 2$). (B) Western blot analysis (W) was done on lysates from two different sets of cell lines of Wt and $-/-$ MEF with anti-ERK2 antibody. (C) (Upper panel) Wt and $-/-$ MEF cells were stimulated with 600 $\mu$M of $H_2O_2$ for the indicated times, and p38 kinase assays were performed as described in Materials and Methods. (Lower panel) The assays were quantified using a PhosphorImager (means $\pm$ SD are shown; $n = 2$). (D) Western blot analysis (W) was done on lysates from two different sets of Wt and $-/-$ MEF cell lines with anti-p38 antibody. Experiments were done in duplicate three times with two different sets of cell lines; data from one representative assay are shown.

To further support the idea of the role of these Gab1 inter-actions in cell viability after oxidative injury, we performed transient cotransfections in $-/-$ MEF/Gab1 cells with an empty vector ($-/-$ MEF/Gab1/CTR), an expression vector containing a dominant-negative form of the p85 regulatory subunit of PI3K ($-/-$ MEF/Gab1/DNp85), or an expression vector containing a catalytically inactive form of SHP2 ($-/-$ MEF/Gab1/SHP2 C/S) together with a vector containing a
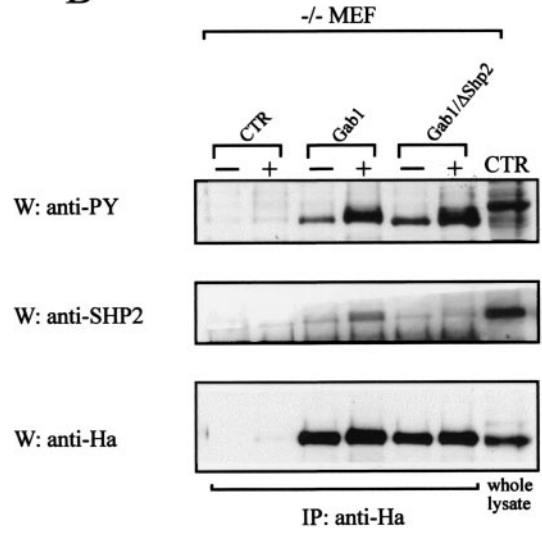
farnesylated form of pEGFP as a reporter of transfection. At 24 h after transfection, the cells were either treated with DMEM (control group) or stimulated with 600 $\mu$M $H_2O_2$ for up to 3 days. The level of cell death was determined by FACS analysis based on the sub-$G_0/G_1$ DNA content of the GFP-positive cells. Figure 7D shows that $-/-$ MEF/Gab1/DNp85 cells are more sensitive to oxidative stress than $-/-$ MEF/Gab1/CTR or $-/-$ MEF/Gab1/SHP2 C/S cells. In contrast to

FIG. 6. Reconstitution of Gab1 expression in $-/-$ MEF cells rescues JNK1 activation after $H_2O_2$ stimulation: dependence on the SHP2 interaction. (A) $-/-$ MEF/CTR, $-/-$ MEF/Gab1, and $-/-$ MEF/Gab1/$\Delta$SHP2 cells were subjected to Western blotting (W) with anti-Gab1 antibody. (B) These cell lines were stimulated with 600 $\mu$M $H_2O_2$ for 10 min, and lysates were used for immunoprecipitation (IP) with anti-HA antibody and to prepare Western blots (W). The blot was incubated with antiphosphotyrosine antibody (anti-PY) or anti-SHP2. The membrane from the upper panel was stripped and reincubated with anti-HA antibody (lower panel). Whole lysate was run as a positive control (CTR) for the antibodies. (C) (Upper panel) $-/-$ MEF/CTR, $-/-$ MEF/Gab1, and $-/-$ MEF/Gab1/$\Delta$SHP2 cells were treated with 600 $\mu$M $H_2O_2$ for 30 min, and JNK1 kinase assays were performed as described in Materials and Methods. (Lower panel) Assays were quantitated using a PhosphorImager (means $\pm$ SD are shown; $n = 2$). (D) Western blot analysis (W) was done on lysates of the cells used in the JNK assay with anti-JNK1 antibody. Using pools of transfected cell lines, the experiments were done in duplicate three times; data from one representative assay are shown.

A

-/- MEF

CTR　　Gab1　　Gab1/ΔShp2

W: anti-Gab1

B

-/- MEF

CTR　　　Gab1　　　Gab1/ΔShp2

−　+　　−　+　　−　+　　CTR

W: anti-PY

W: anti-SHP2

W: anti-Ha

whole
lysate

IP: anti-Ha

C

-/- MEF

CTR　　Gab1　　Gab1/ΔShp2

−　+　−　+　−　+　　H2O2

← GST/c-jun

D

-/- MEF

CTR　Gab1　Gab1/ΔShp2
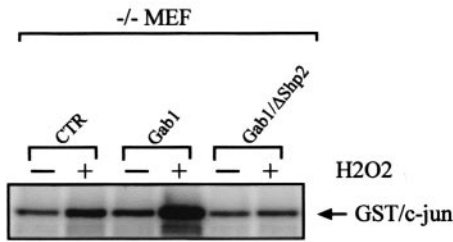
W: anti-JNK1



■ -/- MEF/CTR
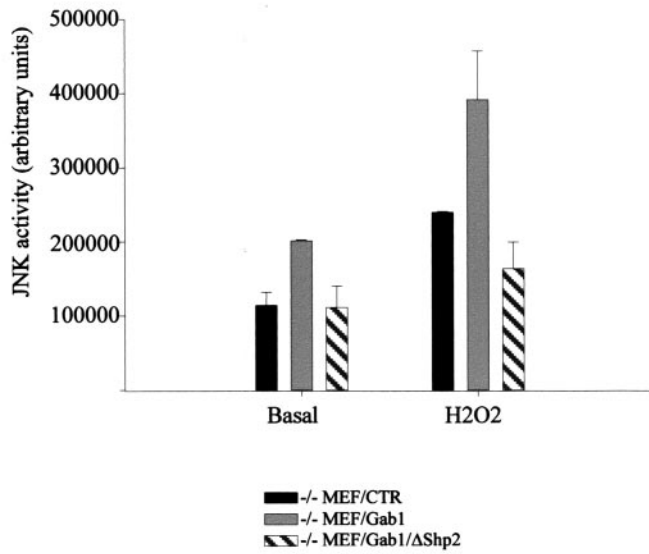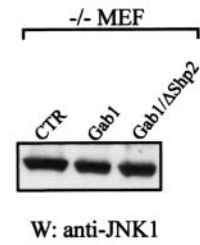▨ -/- MEF/Gab1
▧ -/- MEF/Gab1/ΔShp2

A



B



C



D



FIG. 7. Gab1 has dual roles in cell viability after $H_2O_2$ addition. (A) Wt and $-/-$ MEF cells were seeded in duplicate in 35-mm dishes to attain 80 to 90% confluence 12 to 16 h later. Cells were then either left untreated (DMEM control group) or stimulated with DMEM containing 600 $\mu$M $H_2O_2$ for a period of up to 3 days. Surviving cells (those able to exclude trypan blue) were counted with a hemocytometer. Data are presented as percentages of surviving cells in the treated group relative to the DMEM control group. (B) The same experiment was performed on $-/-$ MEF/CTR, $-/-$ MEF/Gab1, $-/-$ MEF/Gab1/$\Delta$SHP2, $-/-$ MEF/Gab1/$\Delta$PI3K, and Wt MEF cells. (C) $-/-$ MEF/Gab1 and $-/-$ MEF/Gab1/

the other two cell lines, there was an increase in resistance to $H_2O_2$ in $-/-$ MEF/Gab1/SHP2 C/S after the third day, supporting the idea of a role for SHP2 in promoting cell death. These results suggest that Gab1 exerts its role in maintaining cell viability after oxidative stress in a dual fashion, with a positive role through its interaction with PI3K but a negative role through its SHP2 binding.

**Overexpression of Gab1 in $-/-$ MEF/CTR cells increases AKT activation, and this is dependent on its association with PI3K.** As we mentioned above, PI3K/AKT activation in most systems correlates with survival. Since we were able to show that Gab1 exerts a protective role in oxidative stress through its interaction with PI3K, we wanted to explore whether this complex was ultimately responsible for inducing AKT activation. $-/-$ MEF/CTR, $-/-$ MEF/Gab1, $-/-$ MEF/Gab1/$\Delta$PI3K, and $-/-$ MEF/Gab1/$\Delta$SHP2 cells were stimulated for 10 min with $H_2O_2$. Cell lysates were subjected to sodium dodecyl sulfate-polyacrylamide gel electrophoresis, transferred to nitrocellulose, and incubated with anti-phospho-AKT antibody. Figure 8 (upper panel) shows an increase in AKT activation in $-/-$ MEF/Gab1 cells in comparison with that seen in $-/-$ MEF/CTR cells. This increase was not affected in $-/-$ MEF/Gab1/$\Delta$SHP2 cells, but it was abolished in $-/-$ MEF/Gab1/$\Delta$PI3K cells, indicating that the Gab1/PI3K complex is responsible for the activation of this kinase. The lower panel in Fig. 8 shows a similar level of AKT expression in all the cell lines.

## DISCUSSION

The cellular response to oxidative stress is a field of increasing importance. During the last few years there has been an accumulating body of evidence suggesting that the tyrosine kinase receptors and downstream pathways used in growth factor signaling are also shared by oxygen free radical signaling (15). Since Gab1 is a docking protein that is downstream of different growth factor receptors and cytokines (5, 21, 22, 24, 35, 47, 57) and activates many of these same downstream pathways, including PI3K/AKT (21, 22, 34, 35), ERK (57, 65), and JNK (17, 51), we wished to test whether Gab1 can also participate in oxidative stress signaling.

We found that Gab1 becomes tyrosine phosphorylated after $H_2O_2$ stimulation in a dose- and time-dependent manner in different cellular contexts (Fig. 1). Concentrations in the micromolar range are able to induce Gab1 phosphorylation at as early as 5 min, reaching a peak at 10 min and returning to basal levels within 1 h. This kinetics is different from that observed in epithelial cells after EGF stimulation, when the phosphorylation reaches baseline levels in 30 min, or after HGF stimulation, when Gab1 phosphorylation is still maintained for up to

60 min (40). This result shows that there is specificity in the manner by which Gab1 becomes phosphorylated in different signaling pathways, and this may explain differences in subsequent downstream signals.

Having found that Gab1 is tyrosine phosphorylated, we sought to investigate the kinase(s) that can regulate this effect. We elected to use different inhibitors of kinases that have been shown to participate in oxidative stress and induce activation of pathways in which Gab1 is involved. Only PP2, an Src family inhibitor, reduced Gab1 phosphorylation after $H_2O_2$ incubation (Fig. 2), although activation of all these other kinases after $H_2O_2$ addition was found (data not shown). Because PP2 decreased but did not completely abolish the level of Gab1 phosphorylation, other kinases beside Src family members may be involved in this effect. This result demonstrates another example of Src kinase involvement in oxidative injury, since it has been reported that after $H_2O_2$ triggers the phosphorylation of EGFR (8), PLCγ activation (64), JNK activation, and Cas phosphorylation (69) are all dependent on Src. Gab1 phosphorylation is similarly regulated by Src in other systems, such as EGFR signaling (13), lysophosphatidic acid (12), osmotic stress (26), and cell-cell contact signaling (55).

It has been suggested that there is also inactivation of phosphatases in oxidative signaling. It has been shown that $H_2O_2$ can irreversibly inactivate phosphatase 1B in vivo and contribute to EGFR phosphorylation after EGF treatment (36). In this way, the phosphorylation status of Gab1 after $H_2O_2$ can be explained as a result of this balance between kinase activation and inactivation of phosphatases.

As Gab1 functions as a docking protein downstream of several receptor tyrosine kinases (5, 21, 22, 24, 35, 46, 47, 57, 65), we investigated the spectrum of proteins that bind to Gab1 after $H_2O_2$ addition. As shown in Fig. 3, we were able to detect an increase of binding to Gab1 of PI3K, SHP2, and Shc. Gab1 associates with similar proteins following stimulation of cells with EGF, insulin, nerve growth factor, or HGF (21, 22, 40). However, we were unable to detect an increase after $H_2O_2$ triggering in the interaction between Gab1 and PLCγ or Crk, in spite of the formation of these complexes after EGF or HGF addition (19, 21). The induction of different complexes by different stimuli can influence downstream signaling not only by dictating which partners interact but possibly also by serving to target these proteins to a different cellular milieu.

Having showed that Gab1 is tyrosine phosphorylated after $H_2O_2$ addition and recruits several signaling proteins, we were interested in identifying which MAPK pathways are activated. We saw a reduction of JNK activity in Gab1 $-/-$ MEF cells in comparison with that in Wt MEF cells as well as an interme-

---

$\Delta$PI3K cells were stimulated with $H_2O_2$ for 10 min. Lysates were subjected to immunoprecipitation (IP) with anti-HA antibody followed by Western blot analysis (W) with antiphosphotyrosine (anti-PY) or anti-PI3K antibody. The membrane from the upper panel was stripped and reincubated with anti-HA antibody (lower panel). Whole lysate was run as a control for the antibodies (CTR). Using two different cell lines for Wt and $-/-$ MEF and pools for the transfected cell lines, this experiment was done 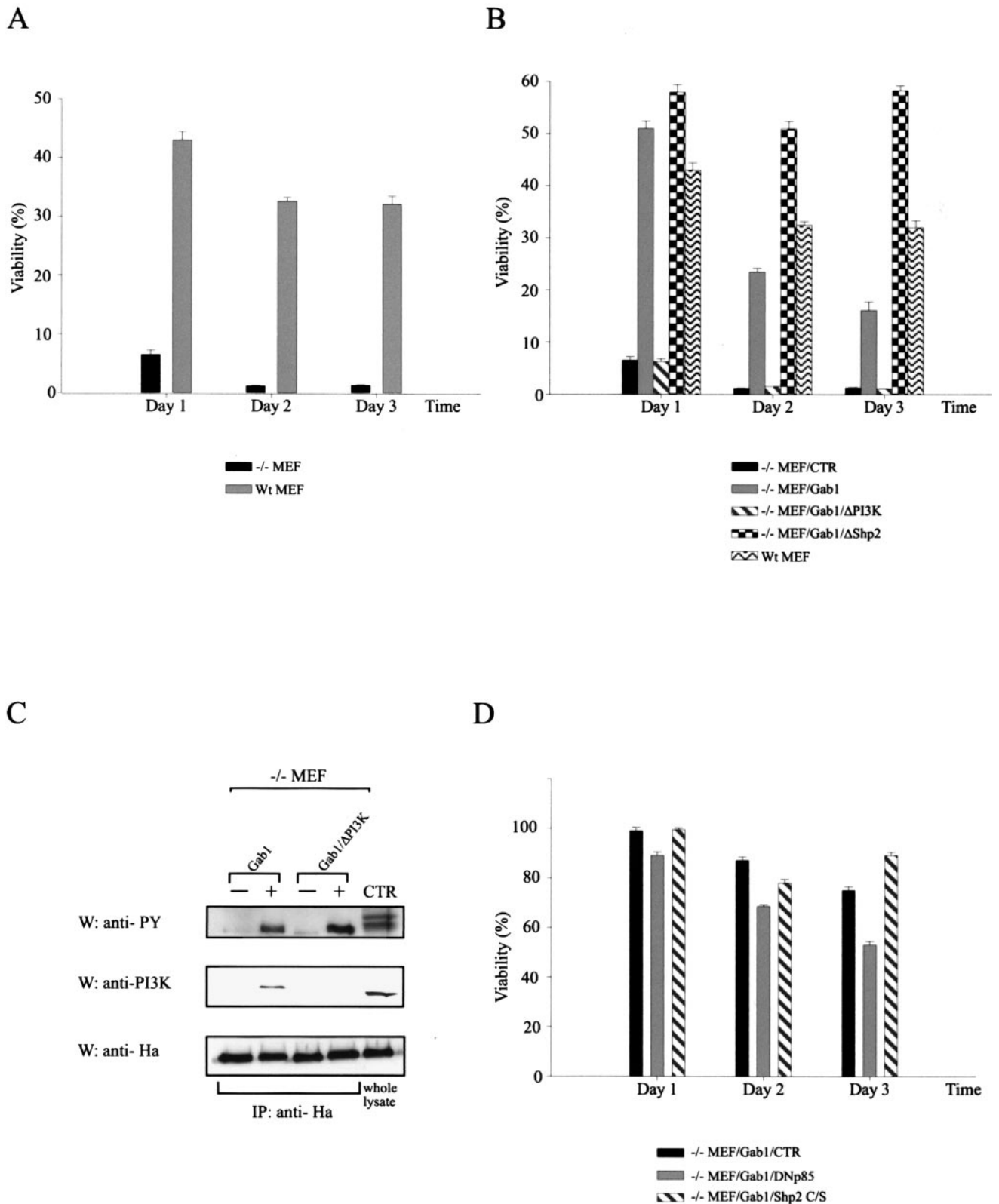in duplicate four separate times. Data from one representative assay are shown. (D) $-/-$ MEF/Gab1 cells were transiently cotransfected with an empty vector ($-/-$ MEF/Gab1/CTR), with an expression vector containing a dominant-negative form of the p85 regulatory subunit of PI3K ($-/-$ MEF/Gab1/DNp85) or with an expression vector containing a catalytically inactive form of SHP2 ($-/-$ MEF/Gab1/SHP2 C/S) together with a vector containing a farnesylated form of pEGFP as a reporter of transfection. At 24 h after transfection, the cells were either treated with DMEM (control group) or stimulated with 600 μM $H_2O_2$ for 3 days. The level of cell death was estimated by FACS analysis based on the sub-$G_0/G_1$ DNA content of the GFP-positive cells. The experiment was done in duplicate two separate times; data from one representative assay are shown.
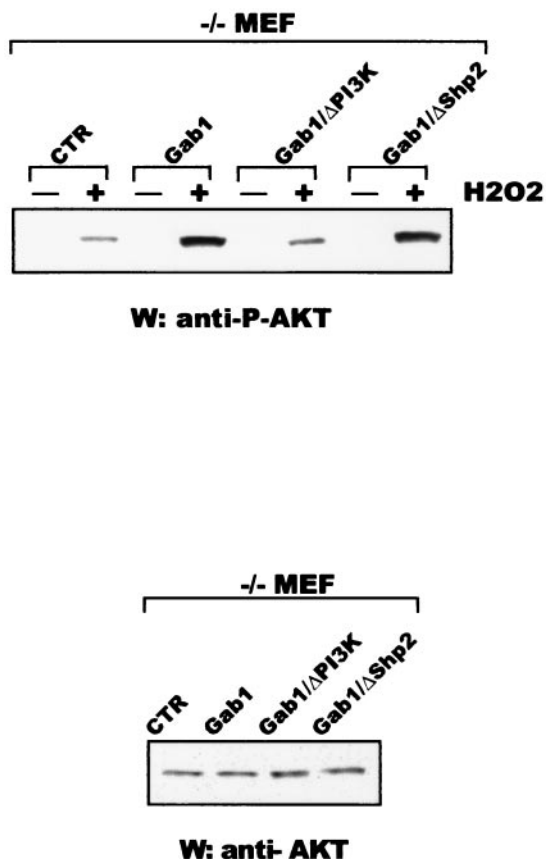
W: anti-P-AKT



W: anti- AKT

FIG. 8. Overexpression of Gab1 in −/− MEF cells increases AKT activation: dependence on the PI3K interaction. −/− MEF/CTR, −/− MEF/Gab1, −/− MEF/Gab1/ΔSHP2, and −/− MEF/Gab1/ΔPI3K cells were stimulated with 600 μM H₂O₂ for 10 min. (Upper panel) Cell lysates were run on a sodium dodecyl sulfate-polyacrylamide gel and subjected to Western blotting analysis (W) using anti-phospho-AKT antibody. (Lower panel) Lysates from the same cell lines were run on a sodium dodecyl sulfate-polyacrylamide gel and incubated with anti-AKT antibody.



FIG. 9. Model depicting the role of Gab1 in oxidative stress. Upon addition of H₂O₂, Src kinases and other kinases (x) sense the signal and become activated and in turn phosphorylate Gab1. Gab1 recruits molecules such as Shc, PI3K, and SHP2. As a result of the Gab1/SHP2 interaction, JNK becomes activated and triggers a death signal. Simultaneously, as a consequence of the Gab1/PI3K association, AKT becomes activated and switches on survival signals. Thus, Gab1 behaves as an integrator of both signals, with a final biological outcome of survival in these experiments.

diate activation in −/+ MEF cells, indicating a dose-dependent effect of Gab1 gene in JNK activation. This result was specific for H₂O₂, since we did not observe differences between these cell lines after treatment with nocodazole, anisomycin, or sorbitol, which are known activators of JNK (Fig. 4) (61, 71). Previously, overexpression studies implied a role for Gab1 in JNK activation downstream of EGFR (51) or Met receptor (17). This is the first report in which homozygous deletion of the Gab1 gene and its reconstitution in −/− MEF cells (−/− MEF/Gab1) (Fig. 6) has revealed an absolute requirement for Gab1 in JNK activation after stress injury. Equally novel is the finding of the role of the Gab1 and SHP2 interaction in JNK activation. It has been reported that in EGF signaling the PH domain of Gab1 and its association with PI3K mediate JNK activation (51) and that in HGF signaling this is mediated through its binding with Crk (17). These results illustrate the specific complexes orchestrated by Gab1 in inducing JNK activation after different stimuli. Other molecules, such as Src, Cas (69), Syk (49), and ASK1 (58), have been reported to be required for JNK activation in oxidative stress, suggesting that
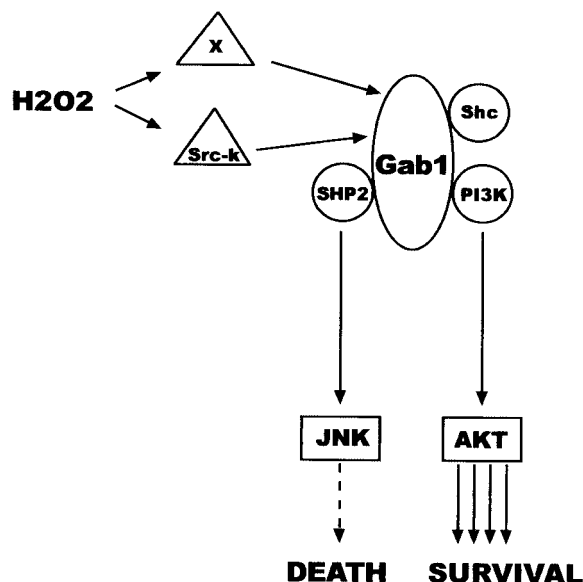
these proteins, together with Gab1, belong to a common pathway that ultimately results in JNK activation.

We sought to investigate the role of Gab1 in the activation of other MAPKs such as p38 and ERK2, which have been shown to be activated after this oxidative stimulus (20, 71). Figure 5 shows that no differences were detected in p38 or ERK2 activation between −/− and Wt MEF cells. This demonstrates that there is specificity in the Gab1 regulation of different MAPKs under different stimuli, since it has been reported that Gab1 is required for ERK2 activation after EGFR, PDGFR, Met, or gp130 activation (25). This may be through differential phosphorylation of Gab1 with various stimuli, since growth factors induce the binding of PLCγ, but we failed to find such an association after H₂O₂ stimulation.

We also examined the biological role of Gab1 in response to stress injury. The Gab1/PI3K interaction with subsequent AKT activation has been shown by us and others to protect PC12 cells or sympathetic neurons from apoptosis induced by serum deprivation (22, 35). We were able to see an enhancement in AKT activation after H₂O₂ addition in −/− MEF/Gab1 cells in comparison with that seen in −/− MEF/CTR cells, and this effect was dependent on a Gab1/PI3K interaction (Fig. 8). In general, the activation of the PI3K/AKT pathway in oxidative stress is associated with protection from apoptosis (14, 63), although some exceptions should be taken into account due to cellular specificity (45).

This is the first report showing that the Gab1/SHP2 interaction plays a negative role in cell survival. We show that this complex is responsible for the induction of JNK activation

after $H_2O_2$ addition. Although there are some contradictory reports on the role of JNK in oxidative stress, the consensus supports a proapoptotic role for JNK after the generation of ROS (3, 4, 31, 59). Interestingly, previous reports have shown that SHP2 has an inhibitory effect on JNK activation after heat shock stress (54) and our results further underscore the context-specific activation of cellular pathways. Since critical substrates of SHP2 have not been identified, it is not clear how it leads to JNK activation, but it has been shown that SHP2 is essential for activation of NF-κB (70).

Under these conditions, our experiments support the idea of an overall role for Gab1 in protection from oxidative stress-induced cell death as the final biological outcome of the activation of two antagonistic pathways: one initiated through its interaction with PI3K and subsequent AKT activation (prosurvival) and the other starting through its binding to SHP2 leading to JNK activation (pro-cell death) (Fig. 9).

This is the first communication describing a role for Gab1 in oxidative stress signaling. The finding of Gab1's participation in oxidative injury adds another piece of information to the concept of cross talk between pathways shared by growth factor, cytokines, GPCR, and oxidative signaling that may contribute to different diseases such as cancer, diabetes, or Alzheimer's. These results also highlight the fact that the activation of specific signaling components and the biological response can be widely divergent according to the stimulus used and the cell context. Thus, it cannot be readily assumed that all signaling pathways are similar. Indeed, our work suggests that all protein interactions and outcomes must be carefully examined for each new stimulus.

## REFERENCES

1. **Aikawa, R., I. Komuro, T. Yamazaki, Y. Zou, S. Kudoh, M. Tanaka, I. Shiojima, Y. Hiroi, and Y. Yazaki.** 1997. Oxidative stress activates extracellular signal-regulated kinases through Src and Ras in cultured cardiac myocytes of neonatal rats. J. Clin. Investig. **100:**1813–1821.
2. **Antonyak, M. A., D. K. Moscatello, and A. J. Wong.** 1998. Constitutive activation of c-Jun N-terminal kinase by a mutant epidermal growth factor receptor. J. Biol. Chem. **273:**2817–2822.
3. **Aoki, H., P. M. Kang, J. Hampe, K. Yoshimura, T. Noma, M. Matsuzaki, and S. Izumo.** 2002. Direct activation of mitochondrial apoptosis machinery by c-Jun N-terminal kinase in adult cardiac myocytes. J. Biol. Chem. **277:**10244–10250.
4. **Behrens, A., M. Sibilia, and E. F. Wagner.** 1999. Amino-terminal phosphorylation of c-Jun regulates stress-induced apoptosis and cellular proliferation. Nat. Genet. **21:**326–329.
5. **Bouscary, D., C. Lecoq-Lafon, S. Chretien, S. Zompi, S. Fichelson, O. Muller, F. Porteu, I. Dusanter-Fourt, S. Gisselbrecht, P. Mayeux, and C. Lacombe.** 2001. Role of Gab proteins in phosphatidylinositol 3-kinase activation by thrombopoietin (Tpo). Oncogene **20:**2197–2204.
6. **Buschmann, T., Z. Yin, A. Bhoumik, and Z. Ronai.** 2000. Amino-terminal-derived JNK fragment alters expression and activity of c-Jun, ATF2, and p53 and increases $H_2O_2$-induced cell death. J. Biol. Chem. **275:**16590–16596.
7. **Chan, T. O., U. Rodeck, A. M. Chan, A. C. Kimmelman, S. E. Rittenhouse, G. Panayotou, and P. N. Tsichlis.** 2002. Small GTPases and tyrosine kinases coregulate a molecular switch in the phosphoinositide 3-kinase regulatory subunit. Cancer Cell **1:**181–191.
8. **Chen, K., J. A. Vita, B. C. Berk, and J. F. Keaney, Jr.** 2001. c-Jun N-terminal kinase activation by hydrogen peroxide in endothelial cells involves SRC-dependent epidermal growth factor receptor transactivation. J. Biol. Chem. **276:**16045–16050.
9. **Chen, Q. M., J. Liu, and J. B. Merrett.** 2000. Apoptosis or senescence-like growth arrest: influence of cell-cycle position, p53, p21 and bax in $H_2O_2$ response of normal human fibroblasts. Biochem. J. **347:**543–551.
10. **Chen, W., J. L. Martindale, N. J. Holbrook, and Y. Liu.** 1998. Tumor promoter arsenite activates extracellular signal-regulated kinase through a signaling pathway mediated by epidermal growth factor receptor and Shc. Mol. Cell. Biol. **18:**5178–5188.
11. **Chevalier, D., E. Thorin, and B. G. Allen.** 2000. Simultaneous measurement of ERK, p38, and JNK MAP kinase cascades in vascular smooth muscle cells. J. Pharmacol. Toxicol. Methods **44:**429–439.
12. **Daub, H., C. Wallasch, A. Lankenau, A. Herrlich, and A. Ullrich.** 1997. Signal characteristics of G protein-transactivated EGF receptor. EMBO J. **16:**7032–7044.
13. **Daub, H., F. U. Weiss, C. Wallasch, and A. Ullrich.** 1996. Role of transactivation of the EGF receptor in signalling by G-protein-coupled receptors. Nature **379:**557–560.
14. **Ding, J., T. Takano, S. Gao, W. Han, C. Noda, S. Yanagi, and H. Yamamura.** 2000. Syk is required for the activation of Akt survival pathway in B cells exposed to oxidative stress. J. Biol. Chem. **275:**30873–30877.
15. **Finkel, T., and N. J. Holbrook.** 2000. Oxidants, oxidative stress and the biology of ageing. Nature **408:**239–247.
16. **Fukunaga, K., T. Noguchi, H. Takeda, T. Matozaki, Y. Hayashi, H. Itoh, and M. Kasuga.** 2000. Requirement for protein-tyrosine phosphatase SHP-2 in insulin-induced activation of c-Jun NH$_2$-terminal kinase. J. Biol. Chem. **275:**5208–5213.
17. **Garcia-Guzman, M., F. Dolfi, K. Zeh, and K. Vuori.** 1999. Met-induced JNK activation is mediated by the adapter protein Crk and correlates with the Gab1-Crk signaling complex formation. Oncogene **18:**7775–7786.
18. **Gonzalez-Rubio, M., S. Voit, D. Rodriguez-Puyol, M. Weber, and M. Marx.** 1996. Oxidative stress induces tyrosine phosphorylation of PDGF alpha- and beta-receptors and pp60c-src in mesangial cells. Kidney Int. **50:**164–173.
19. **Gual, P., S. Giordano, T. A. Williams, S. Rocchi, E. Van Obberghen, and P. M. Comoglio.** 2000. Sustained recruitment of phospholipase C-gamma to Gab1 is required for HGF-induced branching tubulogenesis. Oncogene **19:**1509–1518.
20. **Guyton, K. Z., Y. Liu, M. Gorospe, Q. Xu, and N. J. Holbrook.** 1996. Activation of mitogen-activated protein kinase by $H_2O_2$. Role in cell survival following oxidant injury. J. Biol. Chem. **271:**4138–4142.
21. **Holgado-Madruga, M., D. R. Emlet, D. K. Moscatello, A. K. Godwin, and A. J. Wong.** 1996. A Grb2-associated docking protein in EGF- and insulin-receptor signalling. Nature **379:**560–564.
22. **Holgado-Madruga, M., D. K. Moscatello, D. R. Emlet, R. Dieterich, and A. J. Wong.** 1997. Grb2-associated binder-1 mediates phosphatidylinositol 3-kinase activation and the promotion of cell survival by nerve growth factor. Proc. Natl. Acad. Sci. USA **94:**12419–12424.
23. **Huang, C., Z. Zhang, M. Ding, J. Li, J. Ye, S. S. Leonard, H. M. Shen, L. Butterworth, Y. Lu, M. Costa, Y. Rojanasakul, V. Castranova, V. Vallyathan, and X. Shi.** 2000. Vanadate induces p53 transactivation through hydrogen peroxide and causes apoptosis. J. Biol. Chem. **275:**32516–32522.
24. **Ingham, R. J., M. Holgado-Madruga, C. Siu, A. J. Wong, and M. R. Gold.** 1998. The Gab1 protein is a docking site for multiple proteins involved in signaling by the B cell antigen receptor. J. Biol. Chem. **273:**30630–30637.
25. **Itoh, M., Y. Yoshida, K. Nishida, M. Narimatsu, M. Hibi, and T. Hirano.** 2000. Role of Gab1 in heart, placenta, and skin development and growth factor- and cytokine-induced extracellular signal-regulated kinase mitogen-activated protein kinase activation. Mol. Cell. Biol. **20:**3695–3704.
26. **Janez, A., D. S. Worrall, T. Imamura, P. M. Sharma, and J. M. Olefsky.** 2000. The osmotic shock-induced glucose transport pathway in 3T3-L1 adipocytes is mediated by gab-1 and requires Gab-1-associated phosphatidylinositol 3-kinase activity for full activation. J. Biol. Chem. **275:**26870–26876.
27. **Janssen-Heininger, Y. M., M. E. Poynter, and P. A. Baeuerle.** 2000. Recent advances towards understanding redox mechanisms in the activation of nuclear factor κB. Free Radic. Biol. Med. **28:**1317–1327.
28. **Jin, N., N. D. Hatton, M. A. Harrington, X. Xia, S. H. Larsen, and R. A. Rhoades.** 2000. $H_2O_2$-induced egr-1, fra-1, and c-jun gene expression is mediated by tyrosine kinase in aortic smooth muscle cells. Free Radic. Biol. Med. **29:**736–746.
29. **Johnson, T. M., Z. X. Yu, V. J. Ferrans, R. A. Lowenstein, and T. Finkel.** 1996. Reactive oxygen species are downstream mediators of p53-dependent apoptosis. Proc. Natl. Acad. Sci. USA **93:**11848–11852.
30. **Kalejta, R. F., T. Shenk, and A. J. Beavis.** 1997. Use of a membrane-localized green fluorescent protein allows simultaneous identification of transfected cells and cell cycle analysis by flow cytometry. Cytometry **29:**286–291.
31. **Karin, M., Z. Liu, and E. Zandi.** 1997. AP-1 function and regulation. Curr. Opin. Cell Biol. **9:**240–246.
32. **Kim, H., T. H. Lee, E. S. Park, J. M. Suh, S. J. Park, H. K. Chung, O. Y. Kwon, Y. K. Kim, H. K. Ro, and M. Shong.** 2000. Role of peroxiredoxins in regulating intracellular hydrogen peroxide and hydrogen peroxide-induced apoptosis in thyroid cells. J. Biol. Chem. **275:**18266–18270.
33. **Klotz, L. O., S. M. Schieke, H. Sies, and N. J. Holbrook.** 2000. Peroxynitrite

activates the phosphoinositide 3-kinase/Akt pathway in human skin primary fibroblasts. Biochem. J. **352**(Pt. 1):219–225.

34. **Kojima, H., A. Shinagawa, S. Shimizu, H. Kanada, M. Hibi, T. Hirano, and T. Nagasawa.** 2001. Role of phosphatidylinositol-3 kinase and its association with Gab1 in thrombopoietin-mediated up-regulation of platelet function. Exp. Hematol. **29**:616–622.

35. **Korhonen, J. M., F. A. Said, A. J. Wong, and D. R. Kaplan.** 1999. Gab1 mediates neurite outgrowth, DNA synthesis, and survival in PC12 cells. J. Biol. Chem. **274**:37307–37314.

36. **Lee, S. R., K. S. Kwon, S. R. Kim, and S. G. Rhee.** 1998. Reversible inactivation of protein-tyrosine phosphatase 1B in A431 cells stimulated with epidermal growth factor. J. Biol. Chem. **273**:15366–15372.

37. **Li, Y., J. Liu, and X. Zhan.** 2000. Tyrosine phosphorylation of cortactin is required for $H_2O_2$-mediated injury of human endothelial cells. J. Biol. Chem. **275**:37187–37193.

38. **Mallozzi, C., A. M. Di Stasi, and M. Minetti.** 1999. Activation of src tyrosine kinases by peroxynitrite. FEBS Lett. **456**:201–206.

39. **Marinissen, M. J., M. Chiariello, M. Pallante, and J. S. Gutkind.** 1999. A network of mitogen-activated protein kinases links G protein-coupled receptors to the c-*jun* promoter: a role for c-Jun $NH_2$-terminal kinase, p38s, and extracellular signal-regulated kinase 5. Mol. Cell. Biol. **19**:4289–4301.

40. **Maroun, C. R., M. Holgado-Madruga, I. Royal, M. A. Naujokas, T. M. Fournier, A. J. Wong, and M. Park.** 1999. The Gab1 PH domain is required for localization of Gab1 at sites of cell-cell contact and epithelial morphogenesis downstream from the Met receptor tyrosine kinase. Mol. Cell. Biol. **19**:1784–1799.

41. **Maroun, C. R., M. A. Naujokas, M. Holgado-Madruga, A. J. Wong, and M. Park.** 2000. The tyrosine phosphatase SHP-2 is required for sustained activation of extracellular signal-regulated kinase and epithelial morphogenesis downstream from the Met receptor tyrosine kinase. Mol. Cell. Biol. **20**:8513–8525.

42. **Min, D. S., E. G. Kim, and J. H. Exton.** 1998. Involvement of tyrosine phosphorylation and protein kinase C in the activation of phospholipase D by $H_2O_2$ in Swiss 3T3 fibroblasts. J. Biol. Chem. **273**:29986–29994.

43. **Morimoto, R. I., and M. G. Santoro.** 1998. Stress-inducible responses and heat shock proteins: new pharmacologic targets for cytoprotection. Nat. Biotechnol. **16**:833–838.

44. **Moscatello, D. K., R. B. Montgomery, P. Sundaresan, H. McDanel, M. Y. Wong, and A. J. Wong.** 1996. Transformational and altered signal transduction by a naturally occurring mutant EGF receptor. Oncogene **13**:85–96.

45. **Nemoto, S., and T. Finkel.** 2002. Redox regulation of forkhead proteins through a p66shc-dependent signaling pathway. Science **295**:2450–2452.

46. **Nguyen, L., M. Holgado-Madruga, C. Maroun, E. D. Fixman, D. Kamikura, T. Fournier, A. Charest, M. L. Tremblay, A. J. Wong, and M. Park.** 1997. Association of the multisubstrate docking protein Gab1 with the hepatocyte growth factor receptor requires a functional Grb2 binding site involving tyrosine 1356. J. Biol. Chem. **272**:20811–20819.

47. **Nishida, K., Y. Yoshida, M. Itoh, T. Fukada, T. Ohtani, T. Shirogane, T. Atsumi, M. Takahashi-Tezuka, K. Ishihara, M. Hibi, and T. Hirano.** 1999. Gab-family adapter proteins act downstream of cytokine and growth factor receptors and T- and B-cell antigen receptors. Blood **93**:1809–1816.

48. **Nishida, M., Y. Maruyama, R. Tanaka, K. Kontani, T. Nagao, and H. Kurose.** 2000. G $\alpha$(i) and G $\alpha$(o) are target proteins of reactive oxygen species. Nature **408**:492–495.

49. **Qin, S., Y. Minami, T. Kurosaki, and H. Yamamura.** 1997. Distinctive functions of Syk and Lyn in mediating osmotic stress- and ultraviolet C irradiation-induced apoptosis in chicken B cells. J. Biol. Chem. **272**:17994–17999.

50. **Rao, G. N.** 1996. Hydrogen peroxide induces complex formation of SHC-Grb2-SOS with receptor tyrosine kinase and activates Ras and extracellular signal-regulated protein kinases group of mitogen-activated protein kinases. Oncogene **13**:713–719.

51. **Rodrigues, G. A., M. Falasca, Z. Zhang, S. H. Ong, and J. Schlessinger.** 2000. A novel positive feedback loop mediated by the docking protein Gab1 and phosphatidylinositol 3-kinase in epidermal growth factor receptor signaling. Mol. Cell. Biol. **20**:1448–1459.

52. **Salh, B. S., J. Martens, R. S. Hundal, N. Yoganathan, D. Charest, A. Mui, and A. Gomez-Munoz.** 2000. PD98059 attenuates hydrogen peroxide-in-

duced cell death through inhibition of Jun N-terminal kinase in HT29 cells. Mol. Cell Biol. Res. Commun. **4**:158–165.

53. **Servidei, T., Y. Aoki, S. E. Lewis, A. Symes, J. S. Fink, and S. A. Reeves.** 1998. Coordinate regulation of STAT signaling and c-fos expression by the tyrosine phosphatase SHP-2. J. Biol. Chem. **273**:6233–6241.

54. **Shi, Z. Q., W. Lu, and G. S. Feng.** 1998. The Shp-2 tyrosine phosphatase has opposite effects in mediating the activation of extracellular signal-regulated and c-Jun $NH_2$-terminal mitogen-activated protein kinases. J. Biol. Chem. **273**:4904–4908.

55. **Shinohara, M., A. Kodama, T. Matozaki, A. Fukuhara, K. Tachibana, H. Nakanishi, and Y. Takai.** 2001. Roles of cell-cell adhesion-dependent tyrosine phosphorylation of Gab-1. J. Biol. Chem. **276**:18941–18946.

56. **Sun, X., P. Majumder, H. Shioya, F. Wu, S. Kumar, R. Weichselbaum, S. Kharbanda, and D. Kufe.** 2000. Activation of the cytoplasmic c-Abl tyrosine kinase by reactive oxygen species. J. Biol. Chem. **275**:17237–17240.

57. **Takahashi-Tezuka, M., Y. Yoshida, T. Fukada, T. Ohtani, Y. Yamanaka, K. Nishida, K. Nakajima, M. Hibi, and T. Hirano.** 1998. Gab1 acts as an adapter molecule linking the cytokine receptor gp130 to ERK mitogen-activated protein kinase. Mol. Cell. Biol. **18**:4109–4117.

58. **Tobiume, K., A. Matsuzawa, T. Takahashi, H. Nishitoh, K. Morita, K. Takeda, O. Minowa, K. Miyazono, T. Noda, and H. Ichijo.** 2001. ASK1 is required for sustained activations of JNK/p38 MAP kinases and apoptosis. EMBO Rep. **2**:222–228.

59. **Tournier, C., P. Hess, D. D. Yang, J. Xu, T. K. Turner, A. Nimnual, D. Bar-Sagi, S. N. Jones, R. A. Flavell, and R. J. Davis.** 2000. Requirement of JNK for stress-induced activation of the cytochrome c-mediated death pathway. Science **288**:870–874.

60. **Wagner, B. A., G. R. Buettner, L. W. Oberley, C. J. Darby, and C. P. Burns.** 2000. Myeloperoxidase is involved in $H_2O_2$-induced apoptosis of HL-60 human leukemia cells. J. Biol. Chem. **275**:22461–22469. (Erratum, **276:** 24432, 2001).

61. **Wang, X., M. Gorospe, and N. J. Holbrook.** 1999. gadd45 is not required for activation of c-Jun N-terminal kinase or p38 during acute stress. J. Biol. Chem. **274**:29599–29602.

62. **Wang, X., J. L. Martindale, Y. Liu, and N. J. Holbrook.** 1998. The cellular response to oxidative stress: influences of mitogen-activated protein kinase signalling pathways on cell survival. Biochem. J. **333**:291–300.

63. **Wang, X., K. D. McCullough, T. F. Franke, and N. J. Holbrook.** 2000. Epidermal growth factor receptor-dependent Akt activation by oxidative stress enhances cell survival. J. Biol. Chem. **275**:14624–14631.

64. **Wang, X. T., K. D. McCullough, X. J. Wang, G. Carpenter, and N. J. Holbrook.** 2001. Oxidative stress-induced phospholipase C-gamma 1 activation enhances cell survival. J. Biol. Chem. **276**:28364–28371.

65. **Weidner, K. M., S. Di Cesare, M. Sachs, V. Brinkmann, J. Behrens, and W. Birchmeier.** 1996. Interaction between Gab1 and the c-Met receptor tyrosine kinase is responsible for epithelial morphogenesis. Nature **384**:173–176.

66. **Wheeler, J. C., E. T. Bieschke, and J. Tower.** 1995. Muscle-specific expression of *Drosophila* hsp70 in response to aging and oxidative stress. Proc. Natl. Acad. Sci. USA **92**:10408–10412.

67. **Winnay, J. N., J. C. Bruning, D. J. Burks, and C. R. Kahn.** 2000. Gab-1-mediated IGF-1 signaling in IRS-1-deficient 3T3 fibroblasts. J. Biol. Chem. **275**:10545–10550.

68. **Yang, S.-H., P. R. Yates, A. J. Whitmarsh, R. J. Davis, and A. D. Sharrocks.** 1998. The Elk-1 ETS-domain transcription factor contains a mitogen-activated protein kinase targeting motif. Mol. Cell. Biol. **18**:710–720.

69. **Yoshizumi, M., J. Abe, J. Haendeler, Q. Huang, and B. C. Berk.** 2000. Src and Cas mediate JNK activation but not ERK1/2 and p38 kinases by reactive oxygen species. J. Biol. Chem. **275**:11706–11712.

70. **You, M., L. M. Flick, D. Yu, and G. S. Feng.** 2001. Modulation of the nuclear factor kappa B pathway by Shp-2 tyrosine phosphatase in mediating the induction of interleukin (IL)-6 by IL-1 or tumor necrosis factor. J. Exp. Med. **193**:101–110.

71. **Yujiri, T., S. Sather, G. R. Fanger, and G. L. Johnson.** 1998. Role of MEKK1 in cell survival and activation of JNK and ERK pathways defined by targeted gene disruption. Science **282**:1911–1914.

72. **Zanella, C. L., J. Posada, T. R. Tritton, and B. T. Mossman.** 1996. Asbestos causes stimulation of the extracellular signal-regulated kinase 1 mitogen-activated protein kinase cascade after phosphorylation of the epidermal growth factor receptor. Cancer Res. **56**:5334–5338.